

# Excitation Energy Transfer between Higher Excited States of Photosynthetic Pigments: 1. Carotenoids Intercept and Remove B Band Excitations

Jan P. Götze\* and Heiko Lokstein

Cite This: *ACS Omega* 2023, 8, 40005–40014

Read Online

ACCESS |



Metrics &amp; More

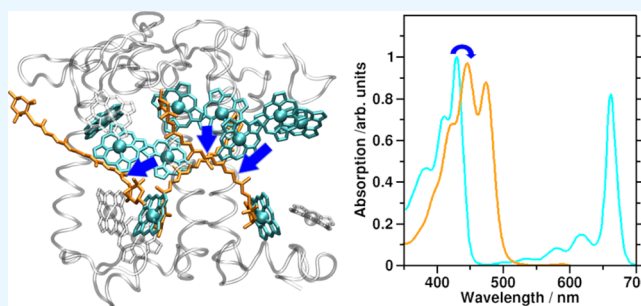


Article Recommendations



Supporting Information

**ABSTRACT:** Chlorophylls (Chls) are known for fast, subpicosecond internal conversion (IC) from ultraviolet/blue-absorbing (“B” or “Soret” states) to the energetically lower, red light-absorbing Q states. Consequently, excitation energy transfer (EET) in photosynthetic pigment–protein complexes involving the B states has so far not been considered. We present, for the first time, a theoretical framework for the existence of B–B EET in tightly coupled Chl aggregates such as photosynthetic pigment–protein complexes. We show that according to a Förster resonance energy transport (FRET) scheme, unmodulated B–B EET has an unexpectedly high range. Unsuppressed, it could pose an existential threat: the damage potential of blue light for photochemical reaction centers (RCs) is well-known. This insight reveals so far undescribed roles for carotenoids (Crts, this article) and Chl *b* (next article in this series) of possibly vital importance. Our model system is the photosynthetic antenna pigment–protein complex (CP29). Here, we show that the B → Q IC is assisted by the optically allowed Crt state ( $S_2$ ): The sequence is B →  $S_2$  (Crt, unrelaxed) →  $S_2$  (Crt, relaxed) → Q. This sequence has the advantage of preventing ~39% of Chl–Chl B–B EET since the Crt  $S_2$  state is a highly efficient FRET acceptor. The B–B EET range and thus the likelihood of CP29 to forward potentially harmful B excitations toward the RC are thus reduced. In contrast to the B band of Chls, most Crt energy donation is energetically located near the Q band, which allows for 74/80% backdonation (from lutein/violaxanthin) to Chls. Neoxanthin, on the other hand, likely donates in the B band region of Chl *b*, with 76% efficiency. Crts thus act not only in their currently proposed photoprotective roles but also as a crucial building block for any system that could otherwise deliver harmful “blue” excitations to the RCs.



## INTRODUCTION

Photosynthesis relies on the absorption and transfer of photon energy by antenna pigments to reaction centers (RCs).<sup>1,2</sup> The key players for absorption and subsequent excitation energy transfer (EET) processes are chlorophylls (Chls).<sup>3–5</sup> Chls remain excited for several ns<sup>6</sup> and use this excitation energy for a productive charge splitting process;<sup>1</sup> this has been the topic of a large number of publications in the past decades.<sup>2,7,8</sup> Chls can thus be ubiquitously found in all photosynthetic antennae (light-harvesting pigment–protein complexes, “LHCs”) and RCs.<sup>2</sup>

Additionally to Chls, carotenoids (Crts) are pigments found in many organisms, with various functions.<sup>9</sup> In photosynthesis, Crts act as (i) structure-stabilizing components and accessory light-harvesting pigments, (ii) Chl triplet excited-state quenchers, and (iii) possibly enabling photoprotection via nonphotochemical quenching (NPQ). NPQ is also assumed to originate from other mechanisms.<sup>10–14</sup> An example of a typical spatial arrangement of Chls and Crts in LHCs is given in Figure 1A.

Despite the importance of Crts, a crucial aspect of Crt photophysics has, so far, not been highlighted: The spectral region in which Crts absorb correlates with the Chls B band absorption (Figure 1B). Chls and Crts exhibit strong absorption in the blue-green spectral region (300 nm and longer wavelengths). Especially for Chl *a* and *b*, in plant systems, the overlap between the spectra is high. For an accessory, light-harvesting pigment, one would rather expect a shifted absorption to cover more of the Chls’ “green gap” (cf., e.g., the phycobiliproteins). Instead, Crts in most organisms containing Chl *a/b* exhibit strong absorption and significant overlap with higher-energy Chl bands. Notably, the Chl B band consists of multiple states.<sup>15</sup> For the sake of simplicity, they are treated as a single entity in the following.

Received: August 10, 2023

Accepted: September 21, 2023

Published: October 16, 2023



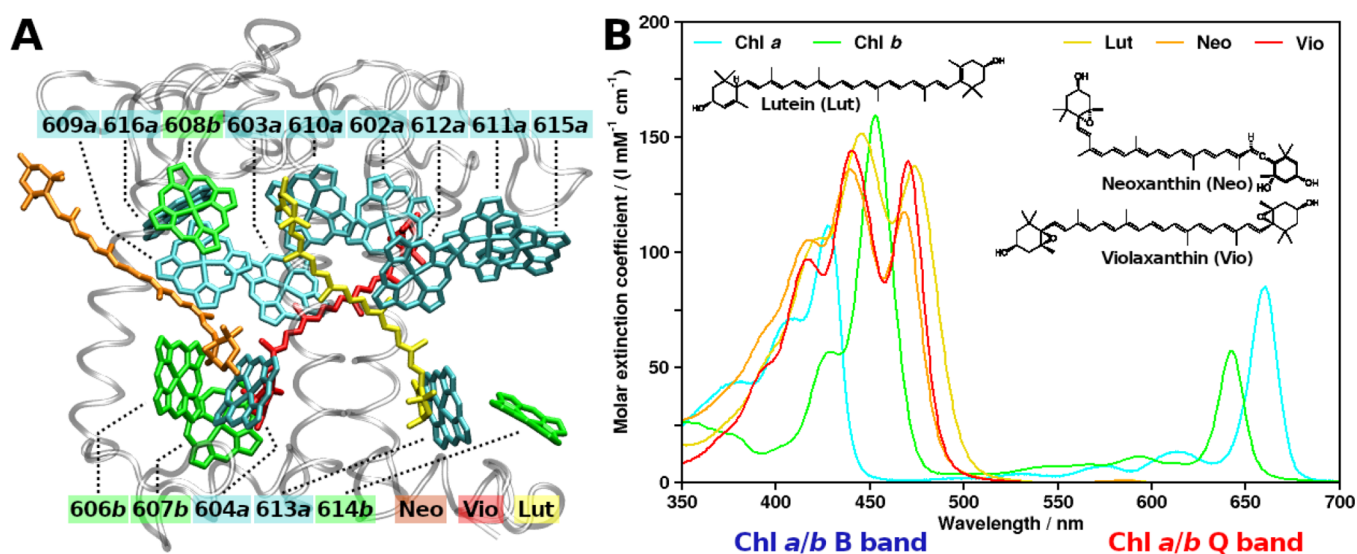


**Figure 1.** Structural arrangement and spectroscopy of typical plant photosynthetic pigments. (A) CP29 complex from *Pisum sativum*, PDB structure 5XNL by Su et al. Viewpoint along the thylakoid membrane plane, looking toward the center of the photosystem II supercomplex. Stromal side at the top and luminal side at the bottom. Protein gray and transparent, Chls a shown as cyan, and Chls b as green (Chl numbering as given in earlier CP29 structures). Crts also shown, lutein in yellow, neoxanthin in orange, and violaxanthin in red. (B) Ultraviolet/visible-region absorption spectra of CP29 pigments (see the text and Table 1 for sources).

In this article, we first aim to assess the possibility of B band EET between Chls. Then, the “competition” between Chls and Crts is explored on the basis of incoherent EET. To keep matters simple, only Förster resonance energy transfer (FRET) theory will be employed.<sup>16,17</sup> In the context of Crts, FRET has the explicit downside that it relies on a point dipole approximation (PDA). For Chls, PDA holds much better than for Crts since Chls are comparatively compact rings, while Crt chromophores are extended chains.<sup>18</sup> The pigments’ “centers” are needed to assign a distance between the transition dipole moments (TDM) for FRET rate calculations (see below). This is thus much less defined for Crts than for Chls.<sup>19</sup> Center-of-mass (COM) distances might in both cases be valid at large separations, but at short distances, PDA based on the COM coordinates becomes less valid, as well. Still, these shortcomings can be managed through exploring the distance limit, and future studies may include more advanced coupling schemes, such as the transition density cube (TDC) approach.<sup>18,20</sup> It is, however, known that, for Chl–Chl coupling, FRET usually underestimates the rates or performs quite well.<sup>19,21–23</sup> In a recent contribution, we have shown that for an ensemble of pigments, such as the LHC studied here, TDC and FRET will, on average, provide nearly identical results.<sup>24</sup> Hence, for a proof of concept, FRET suffices since more elaborately predicted rates should be generally on the same order of magnitude as the rates predicted by FRET.<sup>18,24</sup> FRET further has the distinct advantage of being easily comparable with experimental data. Coherent transport for strongly coupled pigment pairs is also possible but will not be explored here; its occurrence would, however, only strengthen our arguments since it is an additional transport mechanism on a likely ultrafast timescale. Moreover, B state TDMs of Chls are considerably larger than those of the Q states.

The aforementioned spectral competition between Chls and Crts implies the existence of potentially harmful Chl photophysics beyond IC, i.e., B–B excitation energy transfer (EET). As such, the first task of this article is to show that such interactions exist. This is easily done by considering the results

by Leupold and co-workers,<sup>25</sup> who have experimentally shown the corresponding Chl *a/b* B band emission properties. Further, although unmentioned by the authors, Zheng et al. have shown in a theoretical study that coherent B–B EET precedes any B → Q events in a Chl–Chl dimer model (B–B EET lifetime < 10 fs, as seen in Figure 3 of their publication).<sup>26</sup> The results shown below in the present article paint a similar picture, for the first time providing a physical basis and a reason for Crts to prevent B–B EET. Note that the detrimental effects of blue irradiation to the photosynthetic RC are known, with multiple mechanistic proposals.<sup>27–29</sup> It is, however, photophysically of no concern if the high-energy quanta reach the RC via direct irradiation or EET; the effect should be the same.

This article will further investigate the potential of Crt backdonation to Chls, purely on the basis of the “bright” (allowed) Crt state. It has been known for a long time that the vibrational relaxation (VR) of the strongly absorbing Crt state ( $S_2$ ) is very fast (sub-100 fs<sup>30</sup>), and the actual reorganization energy of this process is large for such small changes in molecular geometry.<sup>15,31,32</sup> Despite detectable  $S_2$  emissions of certain Crts, EET processes in plants between Crts and Chls have, to our knowledge, not been attributed to FRET (although shown for bacteriochlorophylls almost 30 years ago<sup>33</sup>). It is well-established that most of the (weak) fluorescence of Crts arises from  $S_2$ , not  $S_1$ .<sup>9</sup> Crts thus intrinsically violate Kasha’s rule,<sup>34,35</sup> and assuming that the  $S_2$  state is a FRET donor seems reasonable.

Consequently, this contribution explores the following: First, the Chl–Chl interactions will be modeled. We will explicitly include all Chl bands, showing that the long-standing neglect of B–B excitation EET may have resulted in a misconception about the Crt role. Second, we will investigate the effect of introducing Chl → Crt EET as a competing element in Chl–Chl interactions. Third, the inverse process (Crt → Chl EET) after Crt VR will also be analyzed.

## METHODS

**FRET Model.** To obtain the FRET rates (in  $\text{ps}^{-1}$ ) between a donor D and an acceptor A,<sup>16,17,36</sup>

$$k_{\text{FRET}} = 8.79 \times 10^{-5} (\kappa^2 \Phi_{\text{f(D)}} J n^{-4} \tau_{\text{D}}^{-1}) / r_{\text{DA}}^6 \quad (1)$$

several excited-state/pigment-specific and conformation-dependent parameters need to be known:  $\kappa$  or  $\kappa^2$  is the orientation factor, with  $\kappa^2$  ranging from 0 to 4, with the value 4 representing perfect alignment of the involved TDMs and pigments.  $\Phi_{\text{f(D)}}$  is the fluorescence yield of the donor state, and  $J$  (in  $\text{M}^{-1} \text{cm}^{-1} \text{nm}^4$ ) is the spectral overlap, for which a variety of different definitions exist (see eq 2).<sup>36,37</sup>  $n$  is the refractive index of the medium (assuming a protein environment,<sup>38</sup> a value of 1.4 is used here), and  $\tau_{\text{D}}$  is the lifetime of the donor state (in ps). Finally,  $r_{\text{DA}}$  is the distance (in Å) between the acceptor and donor compounds using PDA. The Förster radius  $R_0$  is the distance  $r_{\text{DA}}$  at which  $k_{\text{FRET}} = \tau_{\text{D}}^{-1}$ . As already noted above, defining  $r_{\text{DA}}$  between spatially extended compounds such as Crts is not straightforward, and the values computed here for very close pigment pairs must be used with caution.<sup>18</sup> Comparing two compounds of similar character on the basis of FRET is justifiable, as the model can be built such that the actual  $r_{\text{AD}}$  is not relevant (see below).  $J$  can be obtained<sup>17,36</sup> from

$$J = \int_0^\infty \epsilon_{\text{A}}(\lambda) F_{\text{D}}^*(\lambda) \lambda^4 d\lambda \quad (2)$$

in units of  $\text{M}^{-1} \text{cm}^{-1} \text{nm}^4$ , with  $\epsilon_{\text{A}}(\lambda)$  as the molar extinction spectrum of the acceptor (in  $\text{M}^{-1} \text{cm}^{-1}$ ), the wavelength  $\lambda$  (in nm), and the normalized emission spectrum of the donor  $F_{\text{D}}^*(\lambda)$  (in  $\text{nm}^{-1}$ ). For the case presented here, the Chl overall absorption and Q band emission spectra by Li et al.<sup>39</sup> in diethyl ether are used for Chl *a* and *b*; the B band emission of these compounds is taken from Leupold.<sup>25</sup> When restricting the Chl absorbance to either the Q or B band, the bands were separated at 470.5/495 nm for Chl *a/b*. For the spectra of Crts, the corresponding sources are listed in Table 1.

**Table 1. Literature Sources of Crt Spectra Used in This Article with the Corresponding Solvent<sup>a</sup>**

compound (abbreviation)	emission		absorption	
	source ref.	solvent	source ref.	solvent
$\beta$ -carotene (Bcr)	30	<i>n</i> -hexane	(cut at 333.5 nm) <sup>39</sup>	<i>n</i> -hexane
lutein (Lut)	40	<i>n</i> -hexane	15,41	<i>n</i> -hexane
neoxanthin (Neo) <sup>a</sup>	from octaene <sup>42</sup>	EPA, see the source	15,43	ethanol
peridinin (Per)	44	<i>n</i> -hexane	45	<i>n</i> -hexane
violaxanthin (Vio)	46	<i>n</i> -hexane	15	acetone
zeaxanthin (Zea)	46	<i>n</i> -hexane	15	acetone

<sup>a</sup>Neoxanthin emission was unavailable, using octaene instead.

Table 1 contains three Crts present in the CP29 complex (Figure 1A; lutein (Lut, yellow), neoxanthin (Neo, orange), and violaxanthin (Vio, red)). Further,  $\beta$ -carotene (Bcr) is an ubiquitous Crt found in peripheral LHCs as well as the RCs,<sup>47</sup> and zeaxanthin (Zea) is a replacement for Vio under light stress.<sup>32,46</sup> Finally, peridinin (Per) is the primary light-harvesting pigment in the peridinin-chlorophyll *a*-protein (PCP).<sup>10–12,48,49</sup> PCP contains only Per and Chl *a*, with

Chls *a* acting as the connection to the RCs. As such, Per should provide an improved donor capability to Chl *a*, allowing us to validate our model.<sup>10,11,44,50,51</sup>

Finally, a FRET network will be set up, with the Chls and Crts competing as acceptors for excitation energy. For every donor, the total FRET efficiency is computed as

$$E_{\text{FRET, total}} = \frac{\sum_i k_{\text{FRET}, i}}{\tau_{\text{D}}^{-1} + \sum_i k_{\text{FRET}, i}} \quad (3)$$

over all acceptors *i*. Note that  $\tau_{\text{D}}$  is considered to be invariant regardless of the presence of the acceptors.

**Spectral Parameters.** The main advantage of FRET is that it provides a direct connection between the experimentally measured spectral properties of the involved compounds and the EET rate. For the Chl Q band, the required values are well-known, and we take a Q band yield of Chl *a/b* of 0.32/0.117<sup>52</sup> and Q band lifetimes of 6.3/3.2 ns.<sup>6</sup> The most challenging parameters in eq 1 are those that relate to the spectral properties of the higher-energy B states (Chls) and S<sub>2</sub> (Crts) as donors. For those,  $\Phi_{\text{f}}$  and  $\tau_{\text{D}}$  are known to be small, and obtaining exact values requires careful measurements. In the case of Crts, corresponding values could only be found for Bcr in diethyl ether<sup>30</sup> ( $1.50 \times 10^{-4}$  for  $\Phi_{\text{f(Bcr, S}_2\text{)}}$  and 163 fs for  $\tau_{\text{Bcr, S}_2}$ ); however, the variance between Crts in the exact values is small.<sup>9</sup> For the Chl Soret emission/internal conversion (IC), corresponding spectra and values are also only sparsely available.<sup>25,26</sup> While the  $\tau_{\text{D}}$  values for Chl *a/b* could be found as 100/58 fs,<sup>53</sup> the measurements by Leupold and co-workers only allow for an estimate of  $\Phi_{\text{f(Chl, B)}}$  ("less than  $10^{-4}$ ").<sup>25</sup> It is thus prudent to validate these values by other means: a theoretical approach.

It has been known for more than 50 years that the extinction spectrum can be reliably related to the rate of fluorescence via the corresponding Einstein coefficients, if the shape of the fluorescence spectrum is known.<sup>54,55</sup> Then, the expression to obtain the rate of fluorescence, i.e., the Einstein coefficient for spontaneous emission, is

$$k_{\text{f}} = A_{21} = \frac{8\pi c \cdot 2303 n^2}{N_{\text{A}}} \langle \nu^{-3} \rangle^{-1} \int \frac{\epsilon(\nu)}{\nu} d\nu \quad (4)$$

with  $c$  being the speed of light and  $N_{\text{A}}$  as Avogadro's number.  $\nu$  is chosen here instead of  $\lambda$  for unit compatibility (wavenumbers). The resulting rate  $k_{\text{f}}$  is in the time units chosen for  $c$ . Brackets indicate an intensity-weighted average of the fluorescence spectrum. For eq 4, the absorbance of the B band was set to end at  $\nu_{\text{max}} 29700/25450 \text{ cm}^{-1}$  for Chl *a/b*; in contrast, a maximum value is not required for eq 2, as it considers overlaps to emission. The fluorescence yield  $\Phi_{\text{f}}$  can then be obtained via its definition

$$\Phi_{\text{f}} = \frac{k_{\text{f}}}{k_{\text{f}} + \sum k_{\text{IC}}} = \frac{k_{\text{f}}}{\tau_{\text{D}}^{-1}} \quad (5)$$

It may be relevant to note that several of the spectral parameters that we use here are derived from measurements in solution and not for a protein environment. This is a necessary approximation, given that these values are not (yet) available; most other modeling approaches work within the same parameter space. Another issue is the timescale competition between VR and the EET and IC processes; the emission spectra used here seemingly only represent emission from a fully relaxed structure, which might never be reached due to

Table 2. Computed and Experimentally Known<sup>25,30,52</sup> Values for the Fluorescence Yields of Chl and Crt states<sup>a</sup>

band	Chl <i>a</i>		Chl <i>b</i>		Bcr	Lut	Neo	Per	Vio	Zea
	Q	B/10 <sup>-4</sup>	Q	B/10 <sup>-4</sup>						
theory	0.58	2.95	0.27	<b>0.92</b>	3.01	3.02	3.04	1.72	2.64	2.74
exp. <sup>25,30</sup>	<b>0.32</b>	less than 1	0.117	less than 1	1.5	see Bcr				

<sup>a</sup>For Crts, the S<sub>2</sub> state lifetime for Bcr (163 fs) was used in all cases. Bold values are the ones used throughout this article for calculations.

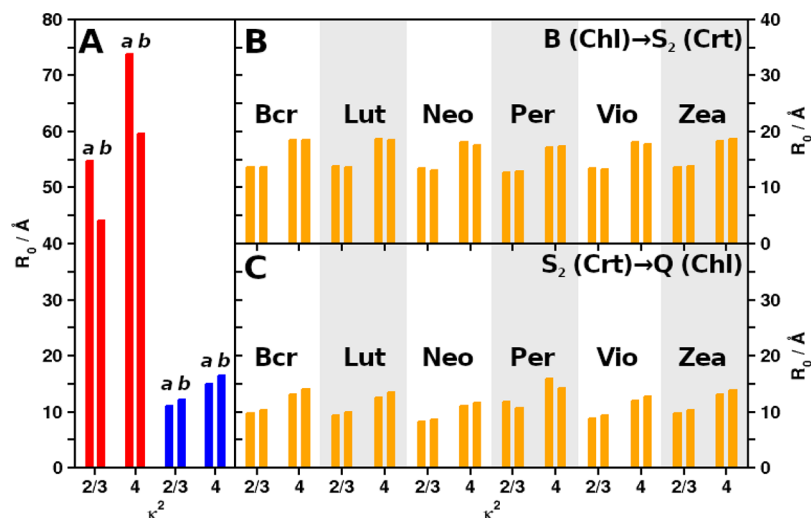


**Figure 2.**  $R_0$  for different values of  $\kappa^2$  and Chls (left/right in each column pair, only indicated in (A)). (A) Chl–Chl homotransfer (red: Q–Q, blue: B–B). (B) FRET from B (Chls) to S<sub>2</sub> (Crts). (C) FRET from S<sub>2</sub> (Crts) to Q (Chls). Fluorescence yields were used as listed in Table 2.

preceding EET or IC. However, for the relevant states investigated in our model (B<sub>x</sub> and S<sub>2</sub>), emission is compared to other ultrafast processes (namely, the IC to Q or S<sub>1</sub>, respectively). Therefore, the spectra used in our model represent the wavelengths available for fluorescence despite the fast IC processes and should represent the wavelengths available for the EET processes well.

Finally, we have to address the choice of representing each Chl band with only one state (B<sub>x</sub> or Q<sub>y</sub>, respectively). To investigate the possibility for B band EET, we need to make sure that EET is not favored by the model itself. Including the “minor” band states would result in higher dipole flexibility and hence likely higher coupling potential,<sup>56</sup> a positive bias that we try to avoid at all times during the present study.

**Structural Model.** The CP29 complex (Figure 1A) will be used as an example, and the corresponding site energies<sup>57</sup> and distance matrices can be found in the Supporting Information (SI, Tables S1, S2 and S3). The site energies have been included as a shift of the Chl *a* or *b* spectra before entering in the calculation of  $J$  (eq 2), while the distances are used in eq 1 directly. Instead of a COM, we use the Mg ion’s position as the location for Chls, and for the Crts, only that the COM results from the atoms in the conjugated carbon chain.

The orientation factors  $\kappa^2$  for the pigments and states in the CP29 model were derived from TDMs that approximately correspond to high-level quantum mechanics calculations.<sup>15,58</sup> Namely, the Chl Q band TDM was associated with the Q<sub>y</sub> state and the B band TDM to the B<sub>x</sub> state, aligned along the Chl atoms NB-ND and C4A-C4C, respectively. For Crt S<sub>2</sub> states, TDMs were aligned along the axis connecting the C12 and C32 atoms (exception: Bcr, C12, and C19 atoms due to different atom numbering; same physical representation).

## RESULTS AND DISCUSSION

**Theoretical Values for the Higher-State Fluorescence Yields.** Equations 4 and 5 provide the fluorescence yields listed in Table 2. The computed values coincide very well with the experimental estimates within the same order of magnitude. To bias against the possibility of the high-energy EET processes investigated here, the lower yield will be used for the following computations (bold in Table 2).

**Q–Q, B–B, and B → S<sub>2</sub> FRET Parameters.** The computed Chl–Chl parameters are listed in Tables S4 of the SI. For the Q–Q homotransfer in Chl *a* and *b*,  $J$  (eq 2) is computed to be 55.1 and 41.7 (in units of 10<sup>14</sup> M<sup>-1</sup> cm<sup>-1</sup> nm<sup>4</sup>), respectively. For the B–B homotransfer, we can expect a lower overlap due to the scaling with  $\lambda^4$ , and indeed, the values are 12.0 for Chl *a* and 24.0 for Chl *b*. When including the full Chl absorption spectra, allowing for B → Q EET, these values increase to 12.1 and 24.4, showing that this interaction can be safely neglected (data not shown). The resulting  $R_0$  Q–Q and B–B values can be found in Figure 2A and Tables S4 of the SI. The model predicts the radii for the Q–Q homotransfer correctly (computed up to 73.8 vs experiment 50–75 Å for Chl *a*).<sup>21,59,60</sup> Using the same approach for the higher-energy B–B transfer (blue columns in Figure 2A), drastically shorter  $R_0$  values are obtained (down to about 1/7 of Q–Q, e.g., 11.1/73.8 for Chl *a*), which would superficially indicate that B–B EET may be less relevant than Q–Q EET. This, however, only holds when considering individual pairs of donors/acceptors. However, before investigating a real system, such as CP29, the FRET parameters for Chl → Crt EET need to be introduced first.

For the Chl → Crt (B → S<sub>2</sub>) EET, the corresponding values can be found in Figure 2B (see Tables S5 in the SI for detailed values). Per as the acceptor is only shown for completeness, it

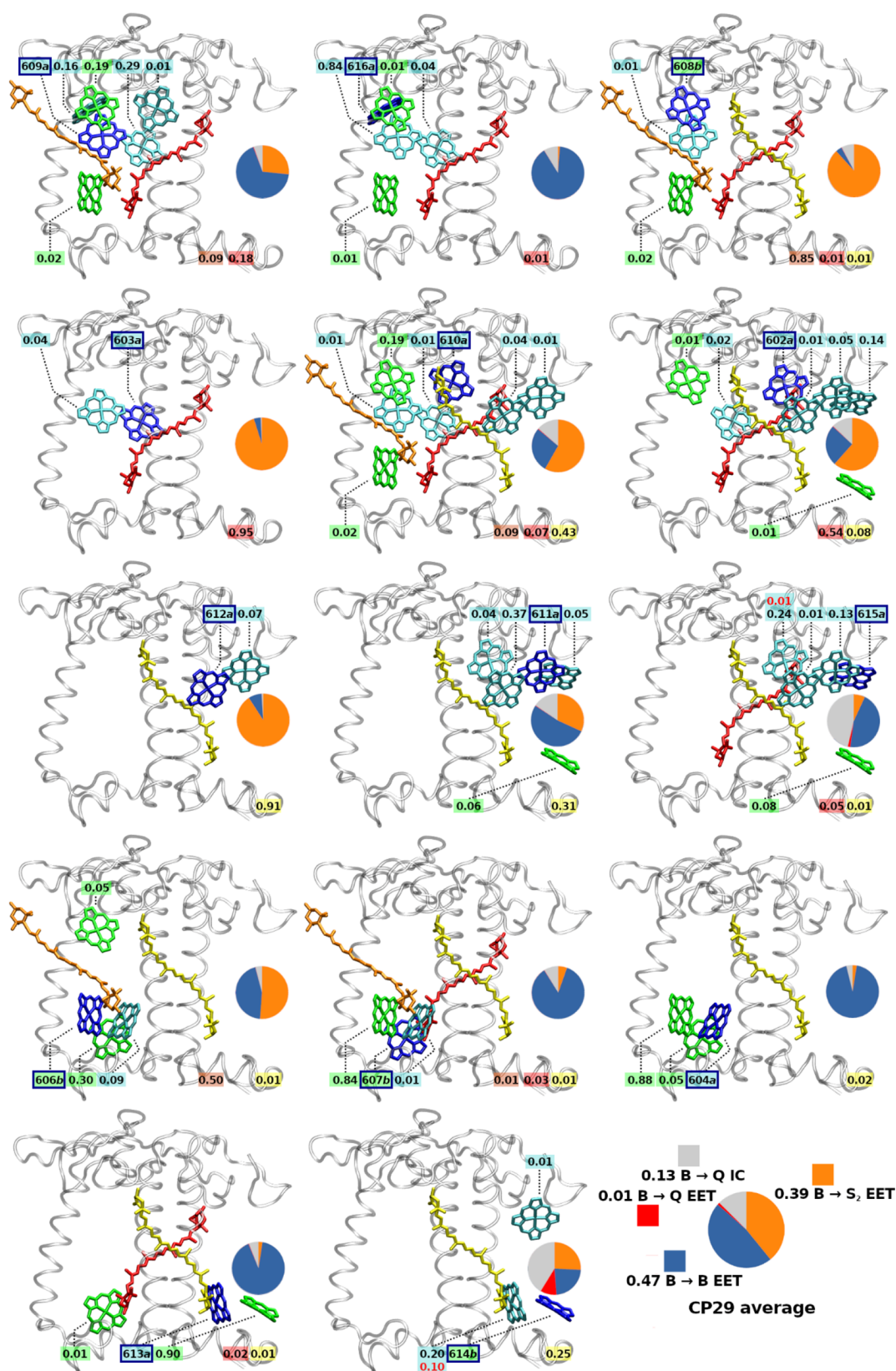


**Figure 3.** Acceptor pigments (rate fraction > 0.005) for FRET B → X processes of B band-excited Chl donors, shown for each Chl in CP29 (donor molecule in dark blue). Acceptor Chls a in cyan, Chl b in green, and Crts in red/orange/yellow (Neo/Vio/Lut).  $E_{\text{FRET, total}}$  for each acceptor from the current donor is shown as black (B → B and B → S<sub>2</sub>) or red (B → Q) numbers. Circles: rate fraction of B → Q internal conversion (IC, gray) vs all FRET B → Q (red), B → B (blue), and B → S<sub>2</sub> EET processes (orange).

is well-known that Per is the main light-harvesting pigment in PCP and acts primarily as a donor, not an acceptor.<sup>10,11,44,50,51</sup>

Regardless, B → S<sub>2</sub> EET exhibits an  $R_0$  of about 13 to 18 Å. The listed values do not differ qualitatively (for a given  $\kappa^2$ ),

although Neo and Vio exhibit a slight preference for Chl *a* as a donor. The strongest preference is Zea (for Chl *b*). Since Vio is replaced by Zea in light-harvesting complex II (LHCII) under light stress,<sup>32,46,61</sup> the different affinities for Chl *a* or *b* to Vio and Zea might be relevant in this context (see also later in this article). Like for the B–B EET, the immediate impression is deceiving: The small differences in  $R_0$  could suggest that the relative coupling differences are small. However, it should be remembered that the EET rates in FRET correlate with  $R_0^6$ , which greatly increases even minute differences.

To pursue this argument, the ratio between the EET rates of two acceptors coupled to the same donor should be considered. The relative efficiency is then

$$E_{\text{rel,A1/A2}} = \frac{k_{\text{f,DA,1}}}{k_{\text{f,DA,2}}} = \frac{R_{0,\text{DA,1}}^6}{R_{0,\text{DA,2}}^6} \quad (6)$$

if  $r_{\text{DA,1}} = r_{\text{DA,2}}$ . In peripheral light-harvesting complexes, Lut is the most prevalent Crt.<sup>47</sup> Considering a competing situation between Lut and Chl *a*,  $E_{\text{rel,Lut/Chl a}}$  would become  $13.8^6/11.1^6 = 3.69$  (for  $\kappa^2 = 2/3$ ). This means that a small difference of 2.7 Å in  $R_0$ , as depicted in Figure 2A,B for  $B \rightarrow B/S_2$  (Chl *a*/Lut), already results in a nearly 4-fold preference for EET to Lut for a weakly coupled pigment pair.

**B–B EET Range: Well-Distributed Ideal System vs Clustered Arrangements.** The above considerations allow for a tentative estimate of the B–B EET range in an ideally distributed Chl system vs in systems with realistic distances as in LHCs. For an ideally distributed Chl density, we look at the  $C_2S_2M_2$  photosystem II (PSII) supercomplex: out of a total of 288 Chl-like compounds in  $C_2S_2M_2$  PSII, 180 are located on the stromal side.<sup>47</sup> Taking the approximate dimensions of  $15 \times 23 \text{ nm}^2$  for the 5XNL PDB structure, this translates to a stromal layer Chl density of  $0.52/\text{nm}^2$ . Note that the realistic effective density is likely higher, as first, the RC core complex has a large stromal area without any Chls (adding about  $2 \times 3 \text{ nm}^2$  of Chl-free area). Second, antenna Chls are strongly clustered in groups with a much higher density, leading to even more Chl-free space; both errors are, however, partially canceled by considering the layer as a perfect 2D plane, not permitting Chl displacement perpendicular to the plane.

Regardless, when taking a hexagonal grid of Chls with a  $0.52/\text{nm}^2$  density, we obtain an average Mg–Mg nearest neighbor distance of 14.9 Å. For a localized donor B band excitation, applying eqs 1 and 3, as well as assuming  $\kappa^2 = 2/3$  to all neighbors, this would translate to a Chl *a*–Chl *a* B–B EET efficiency of 0.50 (0.51 when also taking the layer of second nearest neighbors into account). Assuming two of the six nearest neighbors to be well-oriented ( $\kappa^2 = 4$ ) increases the efficiency to 0.72. This shows that even at moderately long Mg–Mg distances, it would take 2–4 EET “jumps” before the initial population would decay to below  $1/e$  of its original value, meaning that the lifetime of the B excitation is long enough for about 2–4 EET events.

Realistic distances in LHCs are, however, as low as 9.2 Å; see Tables S2 of the SI, allowing for pairwise efficiencies between 0.75 ( $\kappa^2 = 2/3$ ) and 0.95 ( $\kappa^2 = 4$ ). The latter would translate to population decay to  $1/e$  of the initial value only after 19 jumps. Both the distance and the orientation between the pigments are thus, unsurprisingly, the range-determining factors of B band EET. Given the computed FRET efficiencies, intracomplex B band EET is seemingly unrestricted, or at least unrestricted within chains of closely positioned Chls.

Consequently, it appears that a tight clustering of Chls as found in the LHCs would be detrimental if it were present all the way down to the RCs. Our calculations would predict efficient B band EET for such a case, probably resulting in a damage profile akin to direct irradiation.<sup>27,29,62</sup> Consequently, spatial gaps in the Chl chain, as found between Chl clusters and between complexes, may serve as biologically beneficial B band EET interruptions.

**FRET in the B Band Region of CP29.** As shown in the last section, the smaller B–B and  $B \rightarrow S_2$   $R_0$  values shown in Figure 2 do not allow for a clear statement regarding an EET range that would be valid for all possible structures. We have, however, shown above that tightly packed assemblies may exhibit efficient B band FRET processes. To illustrate an actual B band FRET network, CP29<sup>47</sup> will be used as example, including all B and  $S_2$  interactions (Figure 3, details in Tables S6 of the SI). The displayed ratios between IC (gray) and the two classes of EET processes (to Chls, blue, or to Crts, orange) clearly support two core notions: (i) B–B EET exists and mostly outcompetes  $B \rightarrow \text{QIC}$ . Only the Chl 614 shows an IC larger than the sum of the available B–B processes. For the full CP29, B–B EET would make up 77.7% of all Chl B band processes if not for the presence of Crts. Due to the small  $R_0$ , this can only be explained by either very close distances between individual pairs (see Tables S2 in the SI) or simply the vast number of potential acceptors. It turns out that it is actually a mix of both as individual Chls are located in different protein environments. (ii) A large fraction (39.1% on average) of Chl *a/b* B band excitations is preferentially transferred to Crts. With Crts, the B–B EET fraction is only 47.3% instead of 77.7%. Especially, Chl 602, 603, 608, 610, and 612 would otherwise preferentially perform B–B EET, as the IC ratio is comparatively weak. Some other Chls show nearly a half/half  $B/S_2$  EET distribution (606 and 611) or retain a preference for B–B EET (604, 607, 609, 613, 615, and 616). 614 keeps its IC preference also in the presence of Crts.

Regarding notion (i), some Chls, namely, 603, 608, 610, and 612, donate almost exclusively to Crts. These high efficiencies imply a close distance to a specific Crt (e.g., for Chl 612: Lut, 6.6 Å). For such cases, PDA is probably not sufficient anymore, and the effect might be exaggerated. For Chl 614, the immediate environment apparently does not contain many potential acceptors. This leads to the observed IC prevalence, which in turn also seemingly exaggerates the transfer to the Q band (Figure 3, Chl 614 subgraph). This is only due to model limitations, as CP29 itself is normally part of the PSII supercomplex. The comparatively low B band EET performance of Chl 614 is therefore due to the absence of adjacent complexes, namely LHCII and CP24. For example, including the Bcr of the neighboring CP24 complex in a test calculation (using the parameters for the CP29 Neo binding pocket) increases the fraction of CP29 Chl  $\rightarrow$  Crt EET from 39.1 to 40.2%, just by adding a single additional acceptor. While there are also no immediately obvious differences between Chl *a* or *b* visible in Figure 3, we were able to identify a new specific role for this pigment type; this will, however, be the topic of the next article in this series to remain focused on the Crts here.

It must be noted that the Chl  $\rightarrow$  Crt process comes after an optical filter effect: The strong overlap in absorption spectra (not to be confused with  $J$ ) yields a direct competition between Chls and Crts for any photon that can be absorbed by both the B and  $S_2$  states. This enhances the effective B band depletion by Crts, as it does not matter if a photon is directly

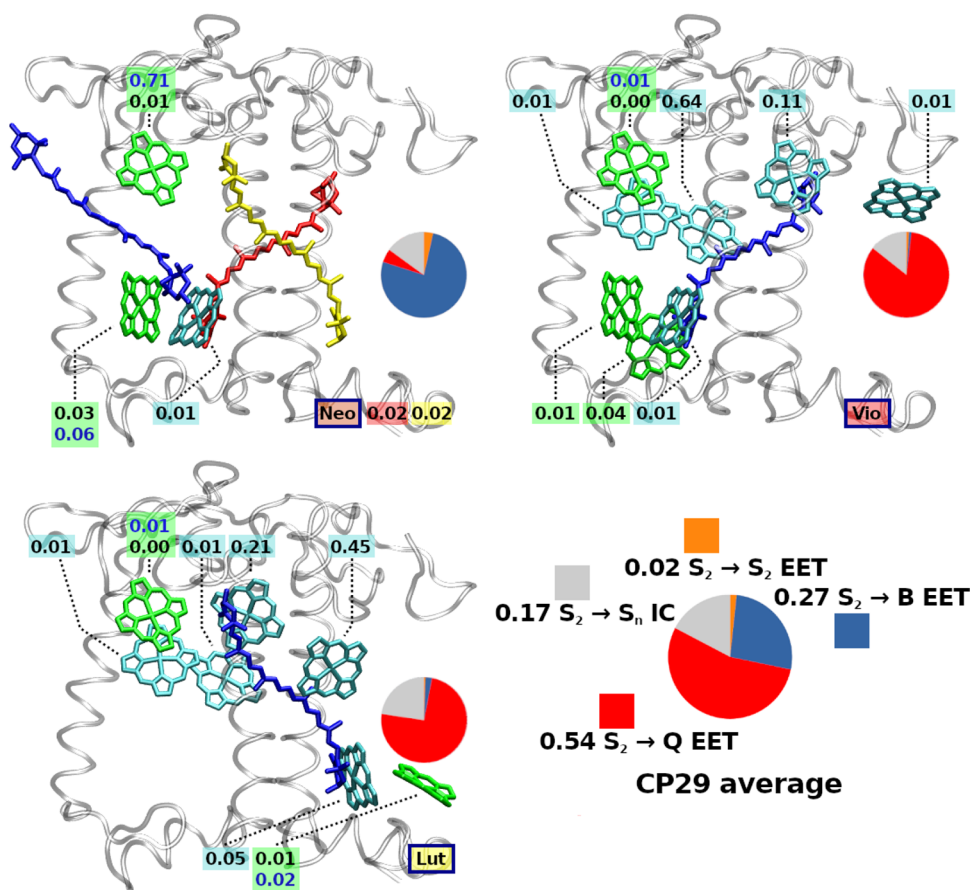


**Figure 4.** Acceptor pigments (rate fraction larger than 0.005) for FRET  $S_2 \rightarrow X$  processes of  $S_2$ -excited Crt donors are shown for each Crt in CP29 (donor molecules in blue). Acceptor Chls a in cyan, Chls b in green, and Crts in red/yellow (Vio/Lut).  $E_{\text{FRET, total}}$  for each acceptor from the current donor is shown as black ( $S_2 \rightarrow Q$  and  $S_2 \rightarrow S_2$ ) or blue ( $S_2 \rightarrow B$ ) numbers. Circles: rate fraction of  $S_2 \rightarrow S_n$  internal conversion (IC, gray) vs all FRET  $S_2 \rightarrow Q$  (red),  $S_2 \rightarrow B$  (blue), and  $S_2 \rightarrow S_2$  EET processes (orange).

absorbed by Crts or if the  $S_2$  excitation is resulting from  $B \rightarrow S_2$  EET; the result is the same. This aspect will also be explored in the next article in this series.<sup>63</sup>

Concluding this section, Crts drastically reduce Chl  $\rightarrow$  Chl B–B FRET processes. This role is facilitated 2-fold, first by direct competition with Chl excitations (a filter effect<sup>64</sup>) and second by competitively depleting Chl B band excitations via EET. The EET competition results in a reduction of Chl B–B EET by a factor of  $1 - (47.3/77.7) = 0.39$  in an isolated CP29 complex. This role explains their ubiquitous presence in the LHCs and RCs, preventing EET of potentially harmful<sup>27–29</sup> B band excitations to the RCs. Further details on this crucial role will be provided at the end of this article.

**$S_2 \rightarrow$  Chl FRET.** An important issue in discussing the potential of backtransfer to Chls from the  $S_2$  of Crts is the energetic location of the Crt  $S_2$  state. Corresponding work has been done extensively in the past, however, often involving a spurious  $S_X$  or the dark  $S_1$  state of Crts.<sup>9,21</sup> The emission spectrum of Crt  $S_2$  is experimentally and theoretically known (Table 1).<sup>15</sup> It should, however, be noted that the experimental 0–0 excitation energies of Crts, typically listed at around 500 nm for the Crts discussed here,<sup>9</sup> do not correspond to the FRET-relevant emission energies. Instead, the overall emission spectrum is relevant, not the energetic location of individual Franck–Condon factors, such as for the 0–0 transition or a maximum intensity. While the adiabatic transition may be important for the photophysical characterization of the Crts,

the mean of the Crt emission spectra is not at all located close to 0–0.<sup>15</sup> The general depiction of  $S_2$  being energetically far from the Chl Q states is thus very misleading in terms of the Crt–Chl FRET capabilities.

Keeping the above in mind, the FRET parameters for a Crt  $\rightarrow$  Chl EET process, from Crt  $S_2$  to Chl, can be found in Table S7 of the SI.  $R_0$  values are shown in Figure 2C. Table S7 of the SI also shows that Crt emission in almost all cases preferentially couples to the Q band, not B (the exception being Neo  $\rightarrow$  Chl b, for which the overlap is evenly shared between B and Q).

All interactions for a Crt–Chl FRET indicate a preference for EET to Chl b instead of Chl a, apart from Per, which is (unsurprisingly<sup>65</sup>) preferring Chl a as an acceptor. The model thus correctly predicts the corresponding biological function of Per. Furthermore, Per is much better suited for backtransfer EET to Chls in general, as shown by the much stronger spectral overlap (from the SI: 12.0/6.2, Chl a/b), as compared to the next strongest donor Crt, Bcr (from the SI: 3.7/5.5). Per, thus, has likely evolved from a primarily B band-depleting pigment to a primarily Q-donating Crt. Among the other Crts, Bcr and Zea are expectedly similar as they are structurally almost identical. The donor ability of the Crts, excluding Per, depends on the length of their conjugated system, which can be easily derived from a particle-in-a-box perspective (short length  $\rightarrow$  higher energies). The resulting order Bcr/Zea  $\rightarrow$  Lut  $\rightarrow$  Vio  $\rightarrow$  Neo applies consistently to the spectra.

From comparing Figure 2B and C, it can be inferred that the backtransfer from Crts should be much less efficient (in a PDA/FRET model) than the EET from the B band to Crts due to the smaller  $R_{0, \text{Crt/Chl}}$  values. However, now with Chls as the acceptors, the radius can be much smaller due to Chls being more numerous. The corresponding results for a CP29 network with Crts as donors can be found in Figure 4 (and Tables S8 in the SI).

The Crt backdonation shows that Lut and Vio basically exhibit the same pattern, with a slightly stronger IC to the Crt dark state ( $S_1$ ) in Lut (22.7% vs 14.3%). In contrast, Neo is primarily coupled to the B state of Chl 608 (71%), which distinguishes this Crt from all the others. This is due to the shorter conjugated chain in Neo compared to Vio or Lut, which raises the emission energies significantly. Again, it must be stressed that CP29 is not an isolated complex; especially, the Neo binding site is located such that one-half of the bound pigment is not inside the CP29 complex but arranged toward other complexes (LHCII in this case). It is thus likely that for a full PSII supercomplex, Neo shows a slightly different coupling pattern.

Despite the Förster radii being much smaller, backdonation from  $S_2$  of Crts to Chl Q states via FRET is found to be similarly efficient to the  $B \rightarrow S_2$  FRET process. Within the PDA, they can do so either by strong individual coupling (e.g., Vio–Chl 603) or by coupling to several different Chl acceptors with a similar preference (e.g., Lut–Chls 610/612).

**Testing the Effect of Crt Replacement: Zea for Vio.** The above calculations were repeated for a slightly modified CP29 model, this time containing Zea instead of Vio (discussed here only in the text for the sake of brevity). Although the replacement is more related to NPQ in LHCII and its specific fourth Crt binding site,<sup>32,46,61</sup> the effects should allow to draw preliminary conclusions for a future LHCII model. The calculation results in  $S_2 \rightarrow Q$  donation rates of Zea being 4.1 times higher than those of Vio. At the same time, the sum of all acceptor rates decreased by a factor of 0.36. Overall coupling patterns (i.e., preferential FRET donors/acceptors) remain identical upon replacement of Vio by Zea in the CP29 model.

Introducing Zea changes the focus from B band coupling to Q band coupling, at least within our model. It remains to be seen if such a change is beneficial under light stress; within the present simulations, no indication is found. For the Zea-induced quenching in CP29 found by Crimi and co-workers,<sup>66</sup> the model presented here is unfortunately not precise enough: the simulated Crts do not differ in  $\tau_{S_2 \rightarrow S_1}$ .

## SUMMARY AND CONCLUSIONS

It is shown that EET is occurring not only between the Chl Q states. Instead, all states with significant TDM participate in EET, even those that undergo rapid IC. This results in Chl B–B EET, which might have detrimental consequences.<sup>27–29</sup>

It is also shown that a simple and efficient solution to the Chl B–B EET problem is the presence of Crts. Crts efficiently compete for Chl B state excitations, both via initial spectral filtering (discussed in detail in the next article of this series<sup>63</sup>) and then through a high likelihood of acting as FRET acceptors (in CP29, at least 39% B–B excitation reduction). Due to rapid internal conversion and their strongly shifted emission spectrum, they cannot donate the energy back into the B band. We have shown that this population can instead

efficiently be donated (by Lut, Vio) into the Chl Q band or rerouted (Neo) to other Chl B bands.

Crts thus provide an important, but so far overlooked, function in photosynthetic light harvesting: rerouting of blue excitations and, as a result, reduction of the B–B EET between Chls.

**Implications.** From an evolutionary perspective, it is interesting to note that even the LHC predecessors, (one-)helical membrane proteins, contain Crt binding sites.<sup>67,68</sup> On the other hand, the problem of B–B EET is definitely distance-dependent (due to the comparatively small  $R_0$  values). It seems that on earlier evolutionary stages, before Chls became tightly clustered, B–B EET may have been simply defused via IC. Crts or other remedies to the B–B EET would only be required to overcome a certain Chl density limit.

There are, however, alternative solutions to the B–B EET problem. One might be simply a high-light-avoiding movement of the organism, but higher plants largely lack this ability. Another one would be a protein-based rerouting mechanism.<sup>57</sup> There might be other related possibilities: For example, bacteriochlorophylls appear to be potential candidates as well since their B band absorption may be less.<sup>69</sup> However, it is commonly assumed that BChls have evolved later as a response to other Chls, harvesting light in other spectral regions to avoid competition by Chls.<sup>70,71</sup>

Finally, there is the explicit possibility that Chl *b* plays a role in the B–B EET context. The next article in this series<sup>65</sup> aims to shed light on a potential new function of Chl *b* as a photoprotective pigment.

## ASSOCIATED CONTENT

### Supporting Information

The Supporting Information is available free of charge at <https://pubs.acs.org/doi/10.1021/acsomega.3c05895>.

CP29 site energies as used for the calculations, CP29 structure distance matrix as used for the calculations, Chl donor FRET parameters, CP29 summed B band process rates, Crt–Chl FRET parameters, and CP29 summed rates for backdonation processes (PDF)

## AUTHOR INFORMATION

### Corresponding Author

Jan P. Götz – *Institut für Chemie und Biochemie, Fachbereich Biologie Chemie Pharmazie, Freie Universität Berlin, 14195 Berlin, Germany*; [orcid.org/0000-0003-2211-2057](https://orcid.org/0000-0003-2211-2057);  
Email: [jan.goetze@fu-berlin.de](mailto:jan.goetze@fu-berlin.de)

### Author

Heiko Lokstein – *Department of Chemical Physics and Optics, Charles University, 121 16 Prague, Czech Republic*;  
[orcid.org/0000-0001-6739-4612](https://orcid.org/0000-0001-6739-4612)

Complete contact information is available at: <https://pubs.acs.org/doi/10.1021/acsomega.3c05895>

### Author Contributions

J.P.G. provided the theoretical concept, calculations, and figures, as well as the initial draft. H.L. provided conceptual guidance and the experimental spectra and edited the draft. Both authors contributed equally to the finalization of the manuscript.

### Notes

The authors declare no competing financial interest.

## ACKNOWLEDGMENTS

J.P.G. gratefully acknowledges funding by the Deutsche Forschungsgemeinschaft (DFG), project number 393271229. H.L. gratefully acknowledges funding by the Czech Science Foundation, GAČR (grant no. 22-17333S). The authors thank Prof. Dr. Peter Saalfrank for his valuable comments on an earlier version of the manuscript. We acknowledge support by the Open Access Publication Fund of the Freie Universität Berlin.

## REFERENCES

- (1) Ferreira, K. N.; Iverson, T. M.; Maghlaoui, K.; Barber, J.; Iwata, S. Architecture of the Photosynthetic Oxygen-Evolving Center. *Science* **2004**, *303*, 1831–1838.
- (2) Lokstein, H.; Renger, G.; Götze, J. Photosynthetic Light-Harvesting (Antenna) Complexes—Structures and Functions. *Molecules* **2021**, *26*, 3378.
- (3) Kuczynska, P.; Jemiola-Rzeminska, M.; Strzalka, K. Photosynthetic Pigments in Diatoms. *Mar. Drugs* **2015**, *13*, 5847–5881.
- (4) Nürnberg, D. J.; et al. Photochemistry beyond the red limit in chlorophyll *f*-containing photosystems. *Science* **2018**, *360*, 1210–1213.
- (5) Graczyk, A.; Żurek, J. M.; Paterson, M. J. On the linear and non-linear electronic spectroscopy of chlorophylls: a computational study. *Photochem. Photobiol. Sci.* **2013**, *13*, 103–111.
- (6) Niedzwiedzki, D. M.; Blankenship, R. E. Singlet and triplet excited state properties of natural chlorophylls and bacteriochlorophylls. *Photosynth. Res.* **2010**, *106*, 227–238.
- (7) Renger, G.; Renger, T. Photosystem II: The machinery of photosynthetic water splitting. *Photosynth. Res.* **2008**, *98*, 53–80.
- (8) Vinyard, D. J.; Ananyev, G. M.; Charles Dismukes, G. Photosystem II: The Reaction Center of Oxygenic Photosynthesis. *Annu. Rev. Biochem.* **2013**, *82*, 577–606.
- (9) Polívka, T.; Sundström, V. Ultrafast Dynamics of Carotenoid Excited States—From Solution to Natural and Artificial Systems. *Chem. Rev.* **2004**, *104*, 2021–2072.
- (10) Götze, J. P.; Karasulu, B.; Patil, M.; Thiel, W. Vibrational relaxation as the driving force for wavelength conversion in the peridinin–chlorophyll *a*-protein. *Biochim. Biophys. Acta, Bioenerg.* **2015**, *1847*, 1509–1517.
- (11) Wagner, N. L.; Greco, J. A.; Enriquez, M. M.; Frank, H. A.; Birge, R. R. The nature of the intramolecular charge transfer state in Peridinin. *Biophys. J.* **2013**, *104*, 1314–1325.
- (12) Krikunova, M.; Lokstein, H.; Leupold, D.; Hiller, R. G.; Voigt, B. Pigment–Pigment Interactions in PCP of *Amphidinium carterae* Investigated by Nonlinear Polarization Spectroscopy in the Frequency Domain. *Biophys. J.* **2006**, *90*, 261–271.
- (13) Kleima, F. J.; et al. Peridinin Chlorophyll *a* Protein: Relating Structure and Steady-State Spectroscopy. *Biochemistry* **2000**, *39*, 5184–5195.
- (14) Ostroumov, E. E.; Götze, J. P.; Reus, M.; Lambrev, P. H.; Holzwarth, A. R. Characterization of fluorescent chlorophyll charge-transfer states as intermediates in the excited state quenching of light-harvesting complex II. *Photosynth. Res.* **2020**, *144*, 171–193.
- (15) Götze, J. P.; Anders, F.; Petry, S.; Witte, J. F.; Lokstein, H. Spectral characterization of the main pigments in the plant photosynthetic apparatus by theory and experiment. *Chem. Phys.* **2022**, *559*, No. 111517.
- (16) May, V.; Kühn, O. *Charge and Energy Transfer Dynamics in Molecular Systems*; Wiley-VCH Verlag GmbH & Co. KGaA, 2011. DOI: 10.1002/9783527633791
- (17) Förster, T. 10th Spiers Memorial Lecture. Transfer mechanisms of electronic excitation. *Discuss. Faraday Soc.* **1959**, *27*, 7–17.
- (18) Krueger, B. P.; Scholes, G. D.; Fleming, G. R. Calculation of Couplings and Energy-Transfer Pathways between the Pigments of LH2 by the ab Initio Transition Density Cube Method. *J. Phys. Chem. B* **1998**, *102*, 5378–5386.
- (19) Beljonne, D.; Curutchet, C.; Scholes, G. D.; Silbey, R. J. Beyond Förster Resonance Energy Transfer in Biological and Nanoscale Systems. *J. Phys. Chem. B* **2009**, *113*, 6583–6599.
- (20) Krueger, B. P.; et al. Energy Transfer in the Peridinin Chlorophyll-*a* Protein of *Amphidinium carterae* Studied by Polarized Transient Absorption and Target Analysis. *Biophys. J.* **2001**, *80*, 2843–2855.
- (21) Croce, R.; van Amerongen, H. Light harvesting in oxygenic photosynthesis: Structural biology meets spectroscopy. *Science* **2020**, *369*, No. eaay2058.
- (22) Jang, S.; Newton, M. D.; Silbey, R. J. Multichromophoric Förster Resonance Energy Transfer from B800 to B850 in the Light Harvesting Complex 2: Evidence for Subtle Energetic Optimization by Purple Bacteria. *J. Phys. Chem. B* **2007**, *111*, 6807–6814.
- (23) Bondarenko, A. S.; Knoester, J.; Jansen, T. L. C. Comparison of methods to study excitation energy transfer in molecular multichromophoric systems. *Chem. Phys.* **2020**, *529*, No. 110478.
- (24) Petry, S.; Tremblay, J. C.; Götze, J. P. Impact of structure, coupling scheme and state of interest on the energy transfer in CP29. *J. Phys. Chem. B* **2023**, *127* (33), 7207–7219.
- (25) Leupold, D.; et al. Two-Photon Excited Fluorescence from Higher Electronic States of Chlorophylls in Photosynthetic Antenna Complexes: A New Approach to Detect Strong Excitonic Chlorophyll *a/b* Coupling. *Biophys. J.* **2002**, *82*, 1580–1585.
- (26) Zheng, F.; Fernandez-Alberti, S.; Tretiak, S.; Zhao, Y. Photoinduced Intra- and Intermolecular Energy Transfer in Chlorophyll *a* Dimer. *J. Phys. Chem. B* **2017**, *121*, 5331–5339.
- (27) Jansen, M. A. K.; Mattoo, A. K.; Edelman, M. D1-D2 protein degradation in the chloroplast. *Eur. J. Biochem.* **1999**, *260*, 527–532.
- (28) Ohnishi, N.; et al. Two-Step Mechanism of Photodamage to Photosystem II: Step 1 Occurs at the Oxygen-Evolving Complex and Step 2 Occurs at the Photochemical Reaction Center. *Biochemistry* **2005**, *44*, 8494–8499.
- (29) Zavafer, A. A theoretical framework of the hybrid mechanism of photosystem II photodamage. *Photosynth. Res.* **2021**, *149*, 107–120.
- (30) Macpherson, A. N.; Gillbro, T. Solvent Dependence of the Ultrafast S<sub>2</sub> – S<sub>1</sub> Internal Conversion Rate of  $\beta$ -Carotene. *J. Phys. Chem. A* **1998**, *102*, 5049–5058.
- (31) Götze, J. P. Vibrational Relaxation in Carotenoids as an Explanation for Their Rapid Optical Properties. *J. Phys. Chem. B* **2019**, *123*, 2203–2209.
- (32) Götze, J. P.; Kröner, D.; Banerjee, S.; Karasulu, B.; Thiel, W. Carotenoids as a Shortcut for Chlorophyll Soret-to-Q Band Energy Flow. *ChemPhysChem* **2014**, *15*, 3392–3401.
- (33) Nagae, H.; Kakitani, T.; Katoh, T.; Mimuro, M. Calculation of the excitation transfer matrix elements between the S<sub>2</sub> or S<sub>1</sub> state of carotenoid and the S<sub>2</sub> or S<sub>1</sub> state of bacteriochlorophyll. *J. Chem. Phys.* **1993**, *98*, 8012–8023.
- (34) Kasha, M. Characterization of electronic transitions in complex molecules. *Discuss. Faraday Soc.* **1950**, *9*, 14.
- (35) Kasha, M.; Rawls, H. R.; Ashraf El-Bayoumi, M. The exciton model in molecular spectroscopy. *Pure Appl. Chem.* **1965**, *11*, 371.
- (36) Qi, Q.; Taniguchi, M.; Lindsey, J. S. Heuristics from Modeling of Spectral Overlap in Förster Resonance Energy Transfer (FRET). *J. Chem. Inf. Model.* **2019**, *59*, 652–667.
- (37) Medintz, I.; Hildebrandt, N. *FRET – Förster Resonance Energy Transfer*; Wiley-VCH Verlag GmbH & Co. KGaA, 2013. DOI: 10.1002/9783527656028.
- (38) Barer, R.; Tkaczyk, S. Refractive Index of Concentrated Protein Solutions. *Nature* **1954**, *173*, 821–822.
- (39) Du, H.; Fuh, R.-C. A.; Li, J.; Corkan, L. A.; Lindsey, J. S. PhotochemCAD: A Computer-Aided Design and Research Tool in Photochemistry. *Photochem. Photobiol.* **1998**, *68*, 141–142.
- (40) Akimoto, S.; et al. Ultrafast Excitation Relaxation Dynamics of Lutein in Solution and in the Light-Harvesting Complexes II Isolated from *Arabidopsis thaliana*. *J. Phys. Chem. B* **2005**, *109*, 12612–12619.
- (41) Zang, L.-Y.; Sommerburg, O.; van Kuijk, F. J. G. Absorbance Changes of Carotenoids in Different Solvents. *Free Radical Biol. Med.* **1997**, *23*, 1086–1089.

- (42) Frank, H. A.; et al. Spectroscopic and Photochemical Properties of Open-Chain Carotenoids. *J. Phys. Chem. B* **2002**, *106*, 2083–2092.
- (43) Cholnokoy, L.; Györgyfy, K.; Szabolcs, J.; Weedon, B. C. L.; Waight, E. S. Folixanthin. *Chem. Commun.* **1966**, *0*, 404–405.
- (44) Zigmantas, D.; Polívka, T.; Hiller, R. G.; Yartsev, A.; Sundström, V. Spectroscopic and Dynamic Properties of the Peridinin Lowest Singlet Excited States. *J. Phys. Chem. A* **2001**, *105*, 10296–10306.
- (45) Zigmantas, D.; Hiller, R. G.; Yartsev, A.; Sundström, V.; Polívka, T. Dynamics of Excited States of the Carotenoid Peridinin in Polar Solvents: Dependence on Excitation Wavelength, Viscosity, and Temperature. *J. Phys. Chem. B* **2003**, *107*, 5339–5348.
- (46) Frank, H. A.; Bautista, J. A.; Josue, J. S.; Young, A. J. Mechanism of Nonphotochemical Quenching in Green Plants: Energies of the Lowest Excited Singlet States of Violaxanthin and Zeaxanthin. *Biochemistry* **2000**, *39*, 2831–2837.
- (47) Su, X.; et al. Structure and assembly mechanism of plant C2S2M2 -type PSII-LHCII supercomplex. *Science* **2017**, *357*, 815–820.
- (48) Schulte, T.; Sharples, F. P.; Hiller, R. G.; Hofmann, E. X-ray structure of the high-salt form of the peridinin-chlorophyll  $\alpha$ -protein from the dinoflagellate *Amphidinium carterae*: Modulation of the spectral properties of pigments by the protein environment. *Biochemistry* **2009**, *48*, 4466–4475.
- (49) Redeckas, K.; Voiciuk, V.; Zigmantas, D.; Hiller, R. G.; Vengris, M. Unveiling the excited state energy transfer pathways in peridinin-chlorophyll  $\alpha$ -protein by ultrafast multi-pulse transient absorption spectroscopy. *Biochim. Biophys. Acta, Bioenerg.* **2017**, *1858*, 297–307.
- (50) Shima, S.; et al. Two-Photon and Fluorescence Spectroscopy and the Effect of Environment on the Photochemical Properties of Peridinin in Solution and in the Peridinin-Chlorophyll-Protein from *Amphidinium carterae*. *J. Phys. Chem. A* **2003**, *107*, 8052–8066.
- (51) Chatterjee, N.; et al. Effect of structural modifications on the spectroscopic properties and dynamics of the excited states of peridinin. *Arch. Biochem. Biophys.* **2009**, *483*, 146–155.
- (52) Weber, G.; Teale, F. W. J. Determination of the absolute quantum yield of fluorescent solutions. *Trans. Faraday Soc.* **1957**, *53*, 646.
- (53) Bricker, W. P.; et al. Non-radiative relaxation of photoexcited chlorophylls: theoretical and experimental study. *Sci. Rep.* **2015**, *5*, 13625.
- (54) Strickler, S. J.; Berg, R. A. Relationship between Absorption Intensity and Fluorescence Lifetime of Molecules. *J. Chem. Phys.* **1962**, *37*, 814–822.
- (55) Birks, J. B.; Dyson, D. J. The relations between the fluorescence and absorption properties of organic molecules. *Proc. R. Soc. London, Ser. A* **1963**, *275*, 135–148.
- (56) Reiter, S.; Bäuml, L.; Hauer, J.; de Vivie-Riedle, R. Q-Band relaxation in chlorophyll: new insights from multireference quantum dynamics. *Phys. Chem. Chem. Phys.* **2022**, *24*, 27212–27223.
- (57) Petry, S.; Götze, J. P. Effect of protein matrix on CP29 spectra and energy transfer pathways. *Biochim. Biophys. Acta, Bioenerg.* **2022**, *1863*, No. 148521.
- (58) Sirohiwal, A.; Berraud-Pache, R.; Neese, F.; Izsák, R.; Pantazis, D. A. Accurate Computation of the Absorption Spectrum of Chlorophyll a with Pair Natural Orbital Coupled Cluster Methods. *J. Phys. Chem. B* **2020**, *124*, 8761–8771.
- (59) Byrdin, M.; Rimke, I.; Schlodder, E.; Stehlik, D.; Roelofs, T. A. Decay Kinetics and Quantum Yields of Fluorescence in Photosystem I from *Synechococcus elongatus* with P700 in the Reduced and Oxidized State: Are the Kinetics of Excited State Decay Trap-Limited or Transfer-Limited? *Biophys. J.* **2000**, *79*, 992–1007.
- (60) van Amerongen, H.; van Grondelle, R. Understanding the Energy Transfer Function of LHCII, the Major Light-Harvesting Complex of Green Plants. *J. Phys. Chem. B* **2001**, *105*, 604–617.
- (61) Young, A. J.; Phillip, D.; Ruban, A. V.; Horton, P.; Frank, H. A. The xanthophyll cycle and carotenoid-mediated dissipation of excess excitation energy in photosynthesis. *Pure Appl. Chem.* **1997**, *69*, 2125.
- (62) Hakala, M.; Tuominen, I.; Keränen, M.; Tyystjärvi, T.; Tyystjärvi, E. Evidence for the role of the oxygen-evolving manganese complex in photoinhibition of Photosystem II. *Biochim. Biophys. Acta, Bioenerg.* **2005**, *1706*, 68–80.
- (63) Götze, J. P.; Lokstein, H. Excitation Energy Transfer between Higher Excited States of Photosynthetic Pigments: 2. Chlorophyll  $b$  is a B Band Excitation Trap. *ACS Omega* **2023**, DOI: 10.1021/acsomega.3c05896.
- (64) Krikunova, M.; et al. Fluorescence of native and carotenoid-depleted LH2 from *Chromatium minutissimum*, originating from simultaneous two-photon absorption in the spectral range of the presumed (optically 'dark') S1 state of carotenoids. *FEBS Lett.* **2002**, *528*, 227–229.
- (65) Schulte, T.; Hiller, R. G.; Hofmann, E. X-ray structures of the peridinin-chlorophyll-protein reconstituted with different chlorophylls. *FEBS Lett.* **2010**, *584*, 973–978.
- (66) Crimi, M.; et al. Time-resolved fluorescence analysis of the recombinant photosystem II antenna complex CP29. Effects of zeaxanthin, pH and phosphorylation. *Eur. J. Biochem.* **2001**, *268*, 260–267.
- (67) Montané, M.-H.; Kloppstech, K. The family of light-harvesting-related proteins (LHCs, ELIPs, HLIPs): was the harvesting of light their primary function? *Gene* **2000**, *258*, 1–8.
- (68) Psencik, J.; Hey, D.; Grimm, B.; Lokstein, H. Photoprotection of Photosynthetic Pigments in Plant One-Helix Protein 1/2 Heterodimers. *J. Phys. Chem. Lett.* **2020**, *11*, 9387–9392.
- (69) Gueymard, C. A. Parameterized transmittance model for direct beam and circumsolar spectral irradiance. *Sol. Energy* **2001**, *71*, 325–346.
- (70) Granick, S. Evolution of Heme and Chlorophyll. In *Evolving Genes and Proteins*; Bryson, V.; Vogel, H. J., Eds.; 67–68 Academic Press, 1965.
- (71) Granick, S. Speculations on the Origins and Evolution of Photosynthesis. *Ann. N. Y. Acad. Sci.* **1957**, *69*, 292–308.